AD-A076 200 NAVAL RESEARCH LAB WASHINGTON DC F/G 20/7
GENERATION OF HIGH ENERGY-HIGH CURRENT ION PULSES BY MAGNETIC C--ETC(U
OCT 79 C A KAPETANAKOS
UNCLASSIFIED NRL-MR-4093 NL

1 OF 1
AD
A076200

END
DATE FILMED
11-79
DDC

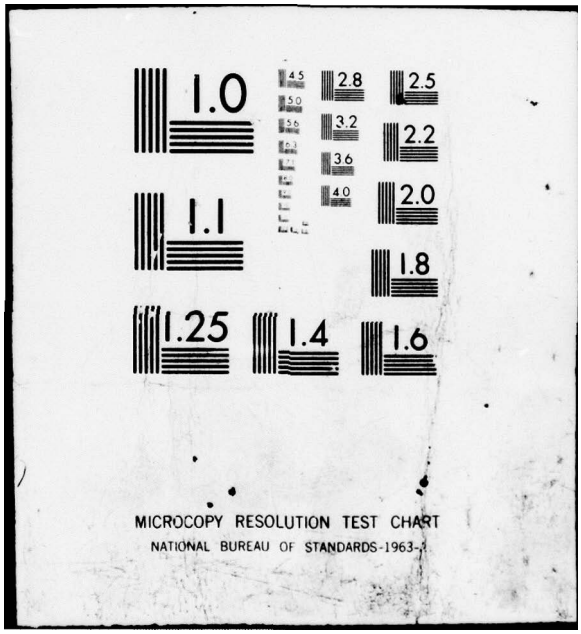
1.0
1.1
1.25
1.4
1.6
1.8
2.0
2.2
2.5
2.8
3.2
3.6
4.0
4.5
5.0
5.6
MICROCOPY RESOLUTION TEST CHART
NATIONAL BUREAU OF STANDARDS-1963-A

NRL Memorandum Report 4093

Generation of High Energy-High Current Ion Pulses by Magnetic Compression of Ion Rings

C. A. Kapetanakos

Experimental Plasma Physics Staff
Plasma Physics Division

LEVEL I

October 24, 1979

NAVAL RESEARCH LABORATORY
Washington, D.C.

SECURITY CLASSIFICATION OF THIS PAGE (When Data Entered)

REPORT DOCUMENTATION PAGE

READ INSTRUCTIONS BEFORE COMPLETING FORM

1. REPORT NUMBER: NRL Memorandum Report 4093	2. GOVT ACCESSION NO.
3. RECIPIENT'S CATALOG NUMBER	
4. TITLE (and Subtitle): GENERATION OF HIGH ENERGY-HIGH CURRENT ION PULSES BY MAGNETIC COMPRESSION OF ION RINGS.	5. TYPE OF REPORT & PERIOD COVERED: Interim report on a continuing NRL problem.
	6. PERFORMING ORG. REPORT NUMBER
7. AUTHOR(s): C. A. Kapetanakos	8. CONTRACT OR GRANT NUMBER(s)
9. PERFORMING ORGANIZATION NAME AND ADDRESS: Naval Research Laboratory, Washington, DC 20375	10. PROGRAM ELEMENT, PROJECT, TASK AREA & WORK UNIT NUMBERS: NRL Problem 67H02-28A
11. CONTROLLING OFFICE NAME AND ADDRESS: Office of Naval Research, Arlington, VA	12. REPORT DATE: October 24, 1979
	13. NUMBER OF PAGES: 33
14. MONITORING AGENCY NAME & ADDRESS (if different from Controlling Office)	15. SECURITY CLASS. (of this report): UNCLASSIFIED
	15a. DECLASSIFICATION/DOWNGRADING SCHEDULE

16. DISTRIBUTION STATEMENT (of this Report)

Approved for public release; distribution unlimited.

NRL-MR-4093

17. DISTRIBUTION STATEMENT (of the abstract entered in Block 20, if different from Report)

18. SUPPLEMENTARY NOTES

This research was supported by the Office of Naval Research and the U.S. Department of Energy.

19. KEY WORDS (Continue on reverse side if necessary and identify by block number)

Ion pulses
Ion rings
Rotating beams

20. ABSTRACT (Continue on reverse side if necessary and identify by block number)

A scheme is proposed for the generation of intense, high energy ion pulses by magnetic compression of ion rings. After compression the ring is extracted through a half magnetic cusp that transforms an appreciable fraction of the ring's rotational energy to translational energy. Using the Vlasov-Maxwell approach, it has been shown the existence of equilibrium of a hollow, rotating beam in the absence of an external magnetic field and a conducting guide tube. Therefore, the proposed scheme appears to be in particular useful for those applications that require a large separation between the accelerator and the target.

DD FORM 1 JAN 73 1473 EDITION OF 1 NOV 65 IS OBSOLETE
S/N 0102-014-6601

SECURITY CLASSIFICATION OF THIS PAGE (When Data Entered)

251 950 LB

CONTENTS

I. Introduction

The inductive acceleration of electrons by adiabatic magnetic compression of electron rings has been demonstrated in several laboratories.[1-4] For weak rings, the observed increase of the mean electron energy and the shrinkage of the major and minor radii of the ring are consistent with the constancy of the magnetic moment $\mu[= P_\perp^2/2m_o B$, where $P_\perp$ is the single particle momentum perpendicular to the magnetic field and B the magnetic field]. A two-hundred fold increase of the electron energy has been observed by Kapetanakos[2] et al., when the time varying magnetic field increased from its initial value of 70 G to 15 kG.

The inductive acceleration of ions by magnetic compression of ion rings is, in principle, very similar to that of the electrons. However, in practice, the ion ring compression is complicated by the presence of space charge neutralizing electrons. These electrons can generate an azimuthal current either by electron-ion drag[5,6], radial electric fields or pressure gradients. Thus, depending on the conditions of the system, at least partial cancellation of the current that is carried by the ions is likely, in particular near the magnetic field null. In some applications partial cancellation of the ion current during magnetic compression is highly desirable because most of the externally supplied energy goes into useful kinetic energy and not into thermal and self-magnetic field energy of the ring.

During the last few years, several models[7-10] have been developed in relation to the magnetic compression of ion rings. The predictions of these theoretical models are sensitive to their basic assumptions. In all these models the dynamics of the neutralizing electrons either have been

Note: Manuscript submitted August 1, 1979.

neglected or treated incompletely.

In a recent publication Sudan[11] has suggested the use of magnetically compressed rings for pellet fusion. In Sudan's scheme the image currents on the walls of the tube that surrounds the ring provide the radial equilibrium during the propagation of the ring from the compression region to the target. The guide tube is destroyed and must be replaced in each shot.

In this report, we propose an alternative scheme for the generation of high energy, high current ion pulses that also is based on the magnetic compression of ion rings.

The basic difference between the present scheme and that of Sudan is on the extraction and the propagation of the ion pulse after compression. The proposed scheme does not require either an external magnetic field or a tube for guiding the ion pulse from the compressor to the target. Therefore, it may be in particular useful in those applications that require an appreciable separation between the compressor or accelerator and the target. In addition, the present approach assumes that the compression of the ion ring is performed in a suitable environment that allows appreciable cancellation of the ion current.

The proposed scheme for the generation of intense, high energy ion pulses by magnetic compression of ion rings is shown schematically in Fig. 1. A hollow, thin ion beam of energy about 2 MeV generated by a low inductance, coaxial reflex tetrode[12] is passed through a magnetic cusp. As a result of the $q(v_z \times B_r)$ force, the ions of the beam obtain azimuthal velocity and start to rotate. The rotational velocity (v_θ) of the ions is further enhanced, at the expense of their translational velocity, by a static, converging magnetic field. The maximum value B_{max} of

the compressing field is such that the protons located at the outer edge of the beam arrive at B_{max} with zero translational velocity.[13] The ion ring is formed by trapping the 50-70 nsec duration ion pulse inside a magnetic mirror with the aid of a gate field.

The rotational energy of the ring is enhanced by increasing in time the confining magnetic field. For adiabatic compression, an appreciable saving in magnetic energy is obtained by using imploding liners.[14] After compression, the ring is extracted out of the confining field by opening the far mirror peak. Initially, the ring is allowed to expand adiabatically in a spatially decreasing field. When the ratio $v_{\parallel}/v_{\perp}$, where $v_{\parallel}, v_{\perp}$ are the velocities of the ring parallel and perpendicular to the field lines respectively, acquires the desired value, the ring is passed through a sharp half cusp that further increases $v_{\parallel}$ at the expense of $v_{\perp}$. Although the radius of the beam remains virtually unchanged as it passes through the sharp half cusp, the conservation of the canonical angular momentum $P_{\theta}\left[= mrv_{\theta} + \frac{qrA_{\theta}}{c}\right]$ requires a rapid expansion of the beam when $A_{\theta}(r) = 0$. However, for intense rotating beams $A_{\theta}(r) \neq 0$ on the right of the half cusp because $A_{\theta}(r) = A_{\theta}^{ext}(r) + A_{\theta}^{self}(r)$ and $A_{\theta}^{self}(r) \neq 0$, although the externally applied vector potential $A_{\theta}^{ext}(r) = 0$. The existence of equilibrium for a hollow, rotating ion pulse that propagates in the $A_{\theta}^{ext}(r) = 0$ region is shown in Section IV, using the Vlasov-Maxwell equation.

The organization of this report is as follows: The magnetic compression of the ring is discussed very briefly in Section II. The transmission of the ring through the cusp and the target location for the particular case of pellet fusion is presented in Section III. The equilibrium of the

hollow beam in the absence of an externally applied field with and without a conducting tube is discussed in Section IV. Finally, a brief summary of the results is given in Section V.

II. Magnetic Compression of the Ring

Efficient transfer of the externally supplied magnetic energy into particle kinetic energy during magnetic compression of an ion ring requires that the self magnetic field to be appreciably smaller than the applied magnetic field. Under these conditions, the magnetic field lines are open and thus only small electric fields can be sustained. If the Budker's parameter ν ($= NR_o$, where N is the number of ions per unit length and R_o is the ion classical radius) of the ring is not appreciably smaller than unity, the self field can be kept small only if the electron return current partially cancels the ring current. Such an electron current can be driven by a radial electric field, a plasma pressure gradient along the minor radius of the ring or collisions. Among the three, plasma pressure gradients appear to be the most appropriate in the present case. The radial force required for the existence of equilibrium is mainly provided by the magnetic field.

If the self magnetic field of a space charge neutral ring is appreciably smaller than the external field, the kinetic energy of the ions E(t) and the particle current I(t) can be estimated from

$$E(t) = 2E(o)[B(t)/B(o)][\gamma(t)+1]^{-1}, \tag{1}$$

and

$$I(t) = I_o(o)[B(t)/B(o)]\gamma^{-1}(t), \tag{2}$$

where E(0), I(o) and B(o) are the initial values of energy, particle current and magnetic field respectively, B(t) is the value of magnetic field at time t and $\gamma(t)$ the relativistic factor.

The technique of generating high magnetic fields by magnetic flux compression is under investigation for several years. At NRL, large initial diameter (~28 cm), 7-cm long seamless liners of annealed aluminum have successfully imploded and peak magnetic fields in excess of 1.3 M gauss have been obtained. In addition, experiments have shown that rotating, hollow cylinders of liquid liners (22% Na, 78% K) can be stably imploded on trapped magnetic flux.

Presently, experiments are underway at NRL to form a strong proton ring. The anticipated parameters of such a ring are shown in Table I. The values of the various parameters after compression, are also shown in the table. In an experiment, the values of the various parameters at the peak of the compression will not be much different than those given in Table I when the self magnetic field is small in comparison with the externally applied field.

III. Extraction of the Ring

After the ring compression is over, the far mirror is switched off and the ring is allowed to propagate adiabatically in a slowly decreasing magnetic field. The velocity of the ring parallel to the magnetic field lines at point 1 (cusp entrance) is given by

$$v_{\parallel 1} = v_{10}(1-B_1/B_m)^{1/2}, \qquad (3)$$

where v_{10} is the azimuthal ring velocity at the end of the compression,

B_m is the middle plane value of the compressing field and B_1 is the magnetic field at the entrance of the cusp. The ratio B_1/B_m is mainly dictated by the maximum ion pulse radius that can be tolerated in a particular application. For example, in pellet irradiation experiments with the parameters of Table 1, $B_1/B_m = 1/2$ appears to be appropriate. In order to further increase v without an appreciable radial expansion, the ion pulse is passed through a half cusp that has a transition width δ_1 that is smaller than the average radius of the gyrating ions.

It is assumed that the cusp is described by the vector potential

$$A_\theta = rzB_1/(2\delta_1) \quad , \quad -\delta_1 \leq z \leq 0 \quad , \tag{4}$$

in a cylindrical coordinates system with its origin as shown in Fig. 1. For a charged particle of mass m and charge q in an axisymmetric field the nonrelativistic Hamiltonian is

$$H = (m/2)(v_r^2 + v_\theta^2 + v_z^2) + q\phi(r) \quad , \tag{5}$$

where $\phi(r)$ is the electrostatic potential and

$$v_\theta = (P_\theta - \frac{qrA_\theta}{c})/mr \quad . \tag{6}$$

The canonical angular momentum P_θ is a constant of the motion and the magnetic vector potential has two components, i.e.,

$$A_\theta(r) = A_\theta^{ext}(r) + A_\theta^{self}(r) \quad .$$

The envelop (boundary) equation for a charged particle in the region $-\delta_1 < z < 0$ can be easily determined when $\phi(r) = A_\theta^{self}(r) = 0$. Substituting Eqs. (4) and (6) into Eq. (5) and taking $P_r = P_z = 0$, the boundary is given by[16]

$$R_{\pm} = 2(\delta_1/z)r_1\{-1\pm[1 + (z/\delta_1)\alpha_1]^{\frac{1}{2}}\}, \tag{7}$$

where $\alpha_1 = P_\theta\Omega_1/H$, $\Omega_1 = qB_1/mc$, $r_1 = (H/2m\Omega_1^2)^{\frac{1}{2}}$, and $P_\theta > 0$ for $q > 0$. Equation (7) shows that crossing of the upper (+ sign) and lower (- sign) boundaries in the region $-\delta_1 < z < 0$ occurs when $1 + (z/\delta_1)\alpha_1 = 0$. Therefore, the boundary remains open and thus a rotating particle can pass through the cusp if

$$\alpha_1^{-1} > 0. \tag{8}$$

According to Eq. (8), a ring that reaches the entrance of the cusp ($z = -\delta_1$) with small self fields and small radial velocity, it passes through provided that

$$(m/2)(v_{\theta_1}^2 + v_{z_1}^2) > R_1\Omega_1(mv_{\theta_1} - qR_1B_1/2), \tag{9}$$

where R_1 is the major radius of the ring at $z = -\delta_1$. Since $v_{\theta 1} \simeq R_1\Omega_1$, Eq. (9) gives

$$v_{z1} > 0, \tag{10}$$

which is not an unexpected result. For $v_{z1} \gg 0$, i.e., for $\alpha_1^{-1} \gg 1$, Eq. (7) becomes

$$R_{\pm}(z) = \begin{matrix} + \\ - \end{matrix}\begin{cases} 0 \\ 4\delta_1 r_1/|z| \end{cases}. \tag{11}$$

The discussion on the transmission of the rotating beam through the half cups is based on the assumption that the self magnetic field of the beam is very small in comparison to the external field. However, the existence of equilibrium in the region that is located to the right of the half cusp ($z > 0$) requires the presence of self fields. Therefore, if the

self magnetic field is zero at the exit of the cusp means muct be found that inhibit the flow of electrons in both the azimuthal and axial directions. Since in multiple elastic scattering the square of the mean scattering angle[17,18] of charged particles injected with the same velocity into neutral gas is proportional to $R_0^2 \, \ell n R_0^{-1}$, where $R_o (= q^2/mc^2)$ is the charged particle classical radius, the electron current can be appreciably inhibited by passing the beam through a neutral gas of appropriate pressure.

The dotted line in Fig. 2 illustrates qualitatively how the field in a linear half cusp is modified by the self field of a long rotating beam. Clearly, the half cusp involves into a full cusp.

The dynamics of a neutralized, rotating ion beam passing through a cusp are very complex. There is experimental evidence[19] that a fraction of the light electrons is tied to the field lines and does not follow the ions across the cusp. The transmission of a rotating beam through a cusp is presently under investigation with a computer simulation code.

For pellet fusion,[20,21] a full cusp may be more desirable than a half cusp. Again, it is assumed that for $z > 0$ the cusp is described by

$$A_\theta = rzB_2/2\delta_2, \quad z > 0 \tag{12}$$

where δ_2 is the transition width and B_2 is the axial magnetic field $B_z = \frac{1}{r}\frac{\partial}{\partial r}(rA_\theta)$ at the exit of the cusp, i.e., of $z = \delta_2$. Similarly to the $z < 0$ case, the boundary equation is

$$R_\mp = 2r_2(\delta_2/z)\left\{\mp 1 + [1 + (z/\delta_2)\alpha_2]^{\frac{1}{2}}\right\}, \quad z > 0 \tag{13}$$

where $\alpha_2 = \alpha_1 B_2/B_1$ and $r_2\alpha_2 = P_\theta/(2mH)^{\frac{1}{2}}$. Figure 3 shows the boundaries of the full cusp for $\alpha_1 = 0.5$ and $\alpha_2 = 0.1$, i.e., for $B_2 = B_1/5$. Higher

values of B_z may be more desirable. A pellet that is located near the exit of the cusp is irradiated not only from the front but also from the back because of the reflected ions. The range of 100 MeV protons in gold is about 0.8 cm and therefore the total diameter of the target (DT and Au) should be ~ 1.7 cm. Thus, heavier ions are more suitable. The size of the pellet can be made compatible with the opening of the boundary by adjusting the value of B_z.

IV. Equilibrium

When a rotating beam that is immersed in a magnetic field is extracted to a free magnetic field region, as in Fig. 1, the canonical angular momentum can only be conserved if r increases, i.e., when an expansion of the beam occurs. For intense rotating beams that are not current neutralized the vector potential $A_\theta(r)$ has two components,

i.e.,

$$A_\theta(r) = A_\theta^{ext}(r) + A_\theta^{self}(r),$$

where $A_\theta^{ext}(r)$ is due to the externally applied field and $A_\theta^{self}(r)$ is due to the azimuthal current of the beam. Therefore, P_θ can be conserved without an appreciable increase of r, even in the absence of an external field, provided that $A_\theta^{self}(r) \neq 0$. However, conservation of P_θ does not warranty the existence of equilibrium. For the equilibrium to exist, a negative force is needed which can be conveniently provided by the self B_θ field.

For a solid rotating beam propagating in the absence of an external magnetic field, the $J_z B_\theta$ force balances the centrifugal and the $J_\theta B_z$ forces. This equilibrium was studied initially by Yoshikawa,[22] who used a cold fluid model ($\nabla P = 0$) and assumed $b \to \infty$ (no surrounding conducting wall).

However, only hollow beams can be efficiently transformed with magnetic cusps. For this reason we study in this section the equilibrium of a hollow beam. Any realistic model dealing with finite thickness hollow beams should include the pressure gradient term. Hot beams ($p \neq 0$) can be conveniently studied using the Vlasov-Maxwell approach.

The present calculation is carried within the Vlasov-Maxwell framework and indicates the existence of equilibrium for a hollow rotating beam, when the external magnetic field is zero and the radius of the conducting guide tube $b \to \infty$.

In addition to these theoretical predictions, recent experiments[23] at NRL have demonstrated the existence of equilibrium for a hollow, overdense, rotating electron beam that propagates inside a conducting guide tube in the absence of an external magnetic field. Presently, experiments are planned to test the existence of equilibrium when the conducting tube that surrounds the beam is removed.

The equilibrium configuration is shown in Fig. 4. It consists of a space charge neutralized, hollow, infinitely long rotating ion beam that is immersed in a uniform magnetic field B_o. The beam is surrounded by a conducting cylindrical liner of radius b and propagates with a velocity $v_z(r)$ along the axial direction. The following simplifying assumptions are made in describing the equilibrium of the propagating ion beam:

(i) Equilibrium properties are azimuthally symmetric and independent of z-coordinate, and

(ii) The equilibrium electric field of the beam is neutralized by an electron background and the current carried by the electrons is equal to zero, i.e., the self magnetic field is generated entirely

by the ions.

Initially, the equilibrium properties of the beam are computed for finite B_o and b. Subsequently, the limited case of $B_o = 0$ and $b \to \infty$ is considered.

The equilibrium is described by the distribution function

$$f^o(H-\omega P_\theta, v_z) = \frac{m\bar{n}}{2\pi} \delta(H-\omega P_\theta - k_1) \delta(v_z + \frac{qA_z}{mc} - \frac{P_{zo}}{m}), \tag{14}$$

where ω, k_1, m, $\bar{n}$, c, m and P_{zo} are constants, $A_z(r)$ is the axial component of the vector potential,

$$H = (m/2)(v_r^2 + v_\theta^2 + v_z^2), \tag{15}$$

$$P_\theta = mrv_\theta + (q/c)rA_\theta(r), \tag{16}$$

and

$$P_z = mv_z + (q/c)A_z(r). \tag{17}$$

The argument of the first delta function in Eq. (14) may be expressed as

$$H - \omega P_\theta - k_1 = (m/2)[(v_\theta - r\omega)^2 + v_r^2] + U_o(r), \tag{18}$$

where

$$U_o(r) = (m/2)[P_{zo}/m - (q/mc)A_z(r)]^2$$

$$- (q/c)rA_\theta(r)\omega - mr^2\omega^2/2 - k_1 < 0. \tag{19}$$

The density profile corresponding to the distribution of Eq. (14) is

$$n(r) = \int f^{o}(H-\omega P_{\theta}, v_z)d^3v = \bar{n}, \quad a_1 \le r \le a_2, \tag{20}$$

where a_1 and a_2 are the roots of $U_o(r)$ defined in (19).

The azimuthal current density is given by

$$J_{\theta}(r) = q\bar{n}V_{\theta}(r), \quad a_1 \le r \le a_2, \tag{21}$$

where $V_{\theta}(r)$ is the mean azimuthal velocity of the rotating beam, i.e.,

$$V_{\theta}(r) = \langle v_{\theta}(r) \rangle = (1/\bar{n})\int v_{\theta} f^{o}(H-\omega P_{\theta}, v_z)d^3v$$

$$= \omega r, \quad a_1 \le r \le a_2. \tag{22}$$

Equation (22) shows that the ion beam rotates with a constant angular velocity ω around its axis of symmetry, i.e., the beam is in a rigid-rotor equilibrium.

The azimuthal component of the magnetic vector potential is determined from

$$\frac{d}{dr}\frac{1}{r}\frac{d}{dr}[rA_{\theta}(r)] = -(4\pi/c)q\bar{n}\omega r, \tag{23}$$

and the axial component from

$$\frac{1}{r}\frac{d}{dr}\left(r\frac{dA_z(r)}{dr}\right) = -(4\pi/c)q\bar{n}[P_{zo}/m - (q/mc)A_z(r)]. \tag{24}$$

The solution of Eq. (23) subject to the boundary conditions that A_{θ} and B_z are continuous at a_1 and a_2 and $\int_0^b 2\pi B_z r dr = \pi b^2 B_o$ (flux conservation) is

$$A_{\theta}(r) = \begin{cases} B_z(a_1)r/2, & 0 \le r \le a_1 \\ B_z(a_1)r/2 - \pi\bar{n}q\omega(r^2-a_1^2)^2/2cr, & a_1 \le r \le a_2 \\ B_z(a_1)r/2 - \pi\bar{n}q\omega[(a_2^2-a_1^2) \\ \quad \times (2r^2-a_1^2-a_2^2)]/2cr, & a_2 \le r \le b, \end{cases} \tag{25}$$

where $B_z(a_1)$ is the axial magnetic field in the inner surface of the beam.

The axial magnetic field $B_z(r) = \frac{1}{r}\frac{d}{dr}(A_\theta r)$ is computed from Eq. (25) and is

$$B_z(r) = \begin{cases} B_0 + \frac{4\pi I_\ell}{c}\left[1 - \frac{(a_1^2 + a_2^2)}{2b^2}\right], & 0 \leq r \leq a \\ B_0 + \frac{4\pi}{c} I_\ell\left[\frac{(a_2^2 - r_2^2)}{(a_2^2 - a_1^2)} - \frac{(a_1^2 + a_2^2)}{2b^2}\right], & a_1 < r < a_2 , \\ B_0 - \frac{4\pi}{c} I_\ell\left[\frac{(a_1^2 + a_2^2)}{2b^2}\right], & a_2 < r \leq b , \end{cases} \tag{26}$$

where $I_\ell = \frac{q\bar{n}\omega}{2}(a_2^2 - a_1^2)$ is the azimuthal current per unit length. For $q > 0$, I_ℓ has the same sign with ω, which is, either negative or positive.

Although the expressions describing the density, azimuthal velocity, $A_\theta(r)$ and $B_z(r)$ appear to be identical to those of reference 24, they are defined in a different region because for the distribution function of Eq. (14), a_1 and a_2 are functions of $A_z(r)$.

The axial component of the vector potential $A_z(r)$ is determined from Eq. (24) and is given by

$$A_z(r) = \begin{cases} 0, \quad 0 \leq r \leq a_1 \\ (cP_{z0}/q)\{1-(a_1/\lambda^*)\left[I_0(r/\lambda^*)K_1(a_1/\lambda^*) + K_0(r/\lambda^*)I_1(a_1/\lambda^*)\right]\}, & a_1<r<a_2, \\ (2I/c)\ell n(a_2/r) + (cP_{z0}/q)\{1-(a_1/\lambda^*)\left[I_0(a_2/\lambda^*)K_0(a_1/\lambda^*) + \right. & \\ \left. K_0(a_2/\lambda^*)I_1(a_1/\lambda^*)\right]\} & \end{cases} \tag{27}$$

where I_n and K_n are modified Bessel functions of order n, $\lambda^* = c/\omega_p$ and $\omega_p^2 = 4\pi\bar{n}q^2/m$. Equation (27) has been derived assuming that A_z and B_θ are continuous at a_1 and a_2 and $A_z(a_1) = B_\theta(a_1) = 0$. The azimuthal magnetic field $B_\theta = -dA_z/dr$ computed from Eq. (27) is

$$B_\theta(r) = \begin{cases} 0, & 0 \le r \le a_1 \\ (4\pi q\bar{n}a_1 P_{zo}/mc)[K_1(a_1/\lambda^*)I_1(r/\lambda^*) - I_1(a_1/\lambda^*)K_1(r/\lambda^*)], & a \le r \le a_2 \\ 2I/cr, & a_2 \le r \le b, \end{cases} \tag{28}$$

where the current of the beam I can be expressed as

$$I = (2\pi q\bar{n}P_{zo}a_1 a_2/m)[K_1(a_1/\lambda^*)I_1(a_2/\lambda^*) - I_1(a_1/\lambda^*)K_1(r/\lambda^*)]. \tag{29}$$

For $a_1/\lambda^* \gg 1$, Eqs. (27), (28) and (29) become

$$A_z(r) = \begin{cases} 0, & 0 \le r \le a_1 \\ (cP_{zo}/q)\{1 - (a_1/r)^{\frac{1}{2}} \cosh[(r-a_1)/\lambda^*]\}, & a_1 \le r \le a_2 \\ (2I/c)\ell n(a_2/r) + (cP_{zo}/q)\left\{1 - (a_1/a_2)^{\frac{1}{2}} \cosh[(a_2-a_1)/\lambda^*]\right\}, & a_2 \le r \le b \end{cases} \tag{30}$$

$$B_\theta(r) = \begin{cases} 0, & 0 \le r \le a_1 \\ (4\pi q\bar{n}\lambda^* P_{zo}/mc)(a_1/r)^{\frac{1}{2}} \sinh[(r-a_1)/\lambda^*], & a_1 \le r \le a_2 \\ 2I/cr, & a_2 \le r \le b, \end{cases} \tag{31}$$

and

$$I = (2\pi q\bar{n}P_{zo}\lambda^*/m)(a_1 a_2)^{\frac{1}{2}} \sinh[(a_2-a_1)/\lambda^*]. \tag{32}$$

Defining the Alfven limiting[25] current I_A as the beam current at which the Larmor radius of a charged particle in the maximum self magnetic field is equal to one-half of the beam radius, we obtain

$$\frac{V_z(a_2)}{(q/mc)(2I_A/a_2 c)} = \frac{a_2}{c}. \tag{33}$$

For $a_1/\lambda^* \gg 1$, Eqs. (30) and (33) give

$$I_A = c^2(P_{zo}/q)(a_1/a_2)^{\frac{1}{2}} \cosh[(a_2 - a_1)/\lambda^*]. \tag{34}$$

Combining Eqs. (32) and (34), we get

$$\frac{I}{I_A} = \frac{a_2}{2\lambda^*} \tanh[(a_2 - a_1)/\lambda^*],$$

which is reduced to

$$\frac{I}{I_A} \simeq a_2/2\lambda^*, \text{ for } (a_2 - a_1)/\lambda^* >> 1 \tag{34}$$

The conclusion from Eq. (34) is that the beam current I can exceed considerably the Alfven current I_A when the collisionless skin depth λ^* is much smaller than the radius[26] and the thickness of the beam.

The function $-U_o(r) > 0$ has a maximum, which can be determined from

$$- \left.\frac{dU_o(r)}{dr}\right|_{r = \rho_o} = 0, \tag{35}$$

Using Eq. (19), Eq. (35) can be written as

$$- (\tfrac{q}{c})v_z(\rho_o)B_\theta(\rho_o) + (\tfrac{q}{c})\omega\rho_o B_z(\rho_o) + m\omega^2\rho_o = 0$$

or

$$- \frac{2\omega}{\Omega_z(\rho_o)} = 1 \mp \left[1 + \frac{4\Omega_\theta(\rho_o)v_z(\rho_o)}{\Omega^2(\rho_o)\rho_o}\right]^{\frac{1}{2}}, \tag{36}$$

where $\Omega_z(\rho_o) = qB_z(\rho_o)/mc$ and $\Omega_\theta = qB_\theta(\rho_o)/mc$. Since the radical in Eq. (36) is greater than unity, the ratio $\omega/\Omega_z(\rho_o)$ can be either positive or negative. Which mode of rotation is present depends upon the initial preparation of the system.

When v_z = const. Eq. (36) gives

$$\omega = - \Omega_z(\rho_o),$$

as expected.[27,28] It can be shown[29] that the pressure P in the beam is

$$P = -\overline{nU}_o(r). \tag{37}$$

Using the 1-fluid equation with $\frac{\partial}{\partial t} = 0$, we obtain

$$\overline{nm}(\vec{V}\cdot\vec{\nabla})\vec{V} = \overline{n}q\,\frac{\vec{V}\times\vec{B}}{c} - \nabla p,$$

or

$$-\frac{V_\theta^2}{r}\,\overline{nm} = (J_\theta B_z - J_z B_\theta)/c - \frac{dP}{dr}. \tag{38}$$

The balance of forces becomes apparent when Eqs. (19) and (37) are inserted in Eq. (38).

The inner a_1 and outer a_2 radii of the beam are the roots of $U_o(r)$ function and therefore $U_o(a_1) = U_o(a_2) = 0$. These radii are in general complicated functions of several parameters. Of particular interest in the present work is the limited case $B_o = 0$ and $b \to \infty$

Defining the layer strength parameter as

$$\nu = \pi\overline{n}q^2(a_2^2 - a_1^2)/mc^2, \tag{39}$$

the constant $B_z(a_1)$ in Eq. (25) can be written as

$$B_z(a_1) = 2\omega mc\nu/q. \tag{40}$$

and the azimuthal component of the vector potential $A_\theta(r)$ in the region $a_1 \leq r \leq a_2$ as

$$A_\theta(r) = (m\omega rc/q)\left[1 - \frac{(r^2-a_1^2)^2}{2r^2(a_2^2-a_1^2)}\right]. \tag{41}$$

Substituting Eqs. (41) and (17) in Eq. (19), it is obtained

$$U_o(r) = U(r) + mv_z^2(r)/2, \tag{42}$$

where

$$U(r) = \frac{\nu w^2 m}{2(a_2^2-a_1^2)} r^4 - \left[\nu + \tfrac{1}{2} + \frac{\nu a_1^2}{(a_2^2-a_1^2)}\right] w^2 m r^2 + \left[\frac{\nu w^2 m}{2(a_2^2-a_1^2)} a_1^4 - k_1\right], \tag{43}$$

and

$$v_z(r) = v_z(a_1)(a_1/\lambda^*)[I_o(r/\lambda^*)K_1(a_1/\lambda^*) + K_o(r/\lambda^*)I_1(a_1/\lambda^*)] \tag{44}$$

The constant $v_z(a_1) = P_{zo}/m$ is the velocity of charged particles in the inner radius of the beam.

The functions $U(r)$ and $-mv_z^2(r)/2$ are sketched in Fig. 6. The two roots a_1^* and a_2^* of $U(r)$ are given by

$$a_{2,1}^{*2} = (1 + \frac{1}{2\nu})(a_2^2 - a_1^2) + a_1^2$$

$$\pm \left\{\left[(1 + \frac{1}{2\nu})(a_2^2-a_1^2) + a_1^2\right]^2 - \left[a_1^4 - 2k_1 \frac{(a_2^2-a_1^2)}{mw^2\nu}\right]\right\}^{\frac{1}{2}}.$$

The maximum value of $U(r)$ occurs at

$$\rho^2 = a_2^2 + (a_2^2 - a_1^2)/2\nu = a_2^2 + (2\pi\bar{n}R_o)^{-1}$$

and is

$$-\frac{U(\rho)}{mw^2(2\nu+1)} = \left[a_1^2(2\nu-1) + a_2^2(2\nu+1)\right]/8\nu + k_1/mw^2(2\nu+1), \tag{45}$$

where $R_o = q^2/mc^2$ is the charged particle classical radius. Necessary conditions for the equilibrium to exist are

$$U(\rho) < 0$$

and

$$|U(\rho)| \geq \frac{m}{2} v_z^2(a_2) \ . \tag{46}$$

Substituting Eqs. (44) and (45) in Eq. (46), it is obtained

$$(2\nu+1)^2 \geq \frac{4\nu v_z^2(a_1)\{(a_1/\lambda^*)^2\left[I_o(a_2/\lambda^*)K_1(a_1/\lambda^*)+K_o(a_2/\lambda^*)I_1/\lambda^*)\right]^2 - 1\}}{\omega^2(a_2^2-a_1^2)} \tag{47}$$

The radii of the beam a_1 and a_2 are the roots of $U_o(r)$ and are determined from Eq. (42). These two radii are given by

$$a_1^2 = (P_{zo}^2 - 2mk_1)/m^2\omega^2(1 + 2\nu), \tag{48}$$

and

$$a_2^2(\nu + 1) + \nu a_1^2 + 2k_1/m\omega^2 =$$

$$\left[v_z^2(a_1)/\omega^2\right](a_1/\lambda^*)^2\left[I_o(a_2/\lambda^*)K_1(a_1/\lambda^*) + K_o(a_2/\lambda^*)I_1(a_1/\lambda^*)\right]^2. \tag{49}$$

When $a_1/\lambda^* >> 1$ and $(a_2 - a_1)/\lambda^* >> 1$, Eq. (49) becomes

$$(a_2-a_1) \approx (\lambda^*/2)\ell n\left\{\frac{a_2\omega^2}{a_1 v_z^2(a_1)}\left[(\nu+1)a_2^2 + \nu a_1^2 + 2k_1/m\omega^2\right]\right\} \ .$$

In order to have $a_2 - a_1 \geq 0$,

$$\left[\omega^2/v_z^2(a_1)\right]\left[(\nu+1)a_2^2 + \nu a_1^2 + 2k_1/m\omega^2\right] \geq a_1/a_2 \ .$$

(b) Infinitesimally thin beam

The various expressions given above are simplified considerably when $a_2 \simeq a_1$, i.e., for very thin beams.

In the thin beam approximation the radial velocity of particles is approximately zero and then

$$\frac{m}{2}v_z^2(r) \approx H - \frac{1}{2}mv_\theta^2 = H - (m/2)\left[P_\theta/mr - (q/mc)A_\theta\right]^2 \qquad (50)$$

Using Eq. (50) and the relation $H - \omega P_\theta = k_1$, Eq. (42) gives

$$a_1^2 \simeq a_2^2 = P_\theta/m\omega(1 + \nu). \qquad (51)$$

Equation (51) can be easily derived from the conservation of $P_\theta = mr^2\dot{\theta} + qA_\theta r/c$. Substituting $\dot{\theta} = \omega$ and using $A_\theta = m\nu\omega rc/q$ from Eq. (41), we get Eq. (51). For $a_1/\lambda^* >> 1$, Eq. (47) becomes

$$(2\nu + 1)^2 \geq 4\pi v_z^2(a_1)\bar{n}R_o\{(a_1/a_2)\cosh^2[(a_2-a_1)/\lambda^*] - 1\}\omega^{-2}.$$

Since

$I = 2\pi q\bar{n}v_z(a_1)\sqrt{a_1 a_2}\lambda^*\sinh[a_2 - a_1)/\lambda^*]$, in the thin beam approximation Eq. (47) becomes

$$(2\nu + 1)\frac{qa_1}{2R_o} \geq (1/\omega). \qquad (52)$$

The above equation shows that in thin beams the current I can be large provided that the frequency of rotation is high.

Equation (52) can be written in a different form. Since $I = q\nu V_z/R_o$ and $\omega a_1 \simeq v_\theta$, Eq. (52) gives

$$\frac{v_\theta}{v_z} \geq \frac{2\nu}{(2\nu + 1)}. \qquad (53)$$

Since for infinitesimally thin beam $\Omega_z(\rho_o) = \omega\nu$ and $\Omega_\theta(\rho_o) = qI/mc^2a_1$, the equation that precedes Eq. (36) gives

$$\frac{v_\theta}{v_z} = \frac{qI}{mc^2a_1(\nu + 1)\omega}, \tag{54}$$

or after substituting for I

$$\frac{v_\theta}{v_z} = \left(\frac{\nu}{1 + \nu}\right)^{\frac{1}{2}} \tag{55}$$

The inequality of Eq. (53) is always satisfied when the equilibrium condition of Eq. (55) is satisfied.

When the distance between the accelerator and the target is much shorter than the beam length, a steady state could be established. Under these conditions, using Eq. (15) with $v_r = o$ and Eqs. (51), (54) and $v_\theta = a_1\omega$, we obtain

$$\frac{(\nu + 1)^2\nu}{(2\nu + 1)} = \frac{P_\theta^2}{2ma_1^2H_p} \equiv \xi, \tag{56}$$

where H_p is the hamiltonian at the peak of the compression. Before the establishment of the steady state, a fraction of the beam energy is invested to build up the magnetic energy. If L is the beam inductance per unit length, then Eq. (56) becomes

$$\frac{(\nu+1)^2\,\nu}{[(2\nu+1) + Lvc^2\,(\nu+1)]} = \frac{P_\theta^2}{2ma_1^2\,H_p} \tag{57}$$

The beam inductance L has two terms, one associated with the rotation and the other with the translation of the beam. In general, L is a function of ν. For an infinitesimally thin beam, of length l, the inductance per unit length is given by

$$L \simeq c^{-2}\left[\, 2\ln(2l/a_1) - 1 + \frac{\nu}{\nu + 1}\,\right]$$

provided $l >> a_1$.

(c) An Example

Combining Eqs. (51), (55) and (56), it is obtained

$$\left(\frac{\mathcal{I} R_o}{q v_{\theta o}}\right) = \frac{\nu^2(\nu+1)}{(2\nu+1)}\,, \tag{58}$$

where $v_{\theta o}$ is the azimuthal velocity of ions at the peak of the compression ($H_p = \frac{1}{2} m v_{\theta o}^2$). Equation (58) determines ν when the value of $\mathcal{I}$ and $v_{\theta o}$ are specified. For $\mathcal{I} = 10^7$A and $H_p = 200$ MeV, Eq. (58) gives $\nu = 0.8$. The value of V_z is determined from $V_z = IR_o/q\nu$ and is 1.19×10^{10} cm/sec. Substituting this value in Eq. (55), we get $V_\theta = 0.8 \times 10^{10}$ cm/sec.

The beam radius is determined from Eq. (51). Using the value of P_θ that corresponds to the values of parameters of Table 1, Eq. (51) gives $a_1 = 0.54$ cm. Since for this particular case the length of the extracted beam is only 38 cm, the ommission of inductive effects is justified only if the target is located a few cm from the exit of the cusp.

In the above example the beam has been assumed to be infinitesimally thin. If the thickness of the beam is finite, the procedure of determining the various parameters of the beam is more complicated. Finally, it should be emphasized that predictions that are based on infinitesimally

thin beams must be treated with care, because such beams are likely to be unstable.

V. Summary

A scheme is proposed for the generation of high energy, high current ion pulses by magnetic compression of ion rings. An important feature of the present scheme is the extraction and unwinding of the ring after compression. The propagation of the extracted pulse from the compression region to the target does not require the presence of metallic boundaries or the application of an external magnetic field. Therefore, such a scheme is in particular useful for targets that are separated from the compressor by a large distance. It appears that the present technique can lead to the generation of hundred of MeV ion pulses without the need for further development in the existing pulse power technology. The capabilities of the proposed scheme appear to be far beyond the present requirements for pellet fusion. However, the successful evolution of the proposed approach to a practical device rests very heavily on several factors, including the formation and stability of ion rings, the stability and finite length of the hollow beam and the ability to inhibit, at least partially, the electron return current in the propagating ion beam.

VI. Acknowledgment

The author is grateful to Drs. A.E. Robson, Phil Sprangle and Jeff Golden for many helpful discussions.

VII. References

1. A.W. Trivelpiece, R.E. Pechacek and C.A. Kapetanakos, Phys. Rev. Lett. 21, 1436 (1968).
2. C.A. Kapetanakos, R.E. Pechacek, D.M. Spero and A.W. Trivelpiece, Phys. Fluids 14, 1555 (1971).
3. S. Ekchouse, Investigation of Nonneutral Magnetically Confined Electron Plasmas, Ph. D. Thesis, Univ. of California, Irvine, 1978.
4. M. Tuszewski, et. al., Proc. of 7th Int. Conf. on Plasma Physics and Contr. Nuclear Fusion Research, Paper # IAEA-CN-37-5-4, Innsbruck, Austria, Aug. 1978.
5. D.E. Baldwin and K.T. Fowler, ILL Report # UCID 17691 (1977).
6. D.E. Baldwin and M.E. Rensink, Electron Effects in Ion-Current Field Reversal, 1978, unpublished.
7. H.H. Fleischmann, Proc. of Electr. and Electromagnetic Confin. of Plasmas, N.Y. (1974).
8. R.N. Sudan and E. Ott, Phys. Rev. Lett. 33, 355 (1974).
9. E.S. Weibel, Phys. of Fluids 20, 1195 (1977).
10. R.V. Lovelace, Kinetic Theory of Ion Ring Compression (unpublished).
11. R.N. Sudan, Phys. Rev. Lett. 41, 476 (1978).
12. J.A. Pasour, R.A. Mahaffey, J. Golden and C.A. Kapetanakos, Phys. Rev. Lett. 40, 448 (1978).
13. C.A. Kapetanakos, J. Golden, A. Drobot, R.A. Mahaffey, S.J. Marsh and J.A. Pasour, Proc. of the 2nd Intern. Top. Conf. on High Power Electron and Ion Beam Research and Technology, Ithaca, N.Y., Oct. 1977.
14. P.J. Turchi and A.E. Robson, Pulsed High Beta Plasma (Pergamon Press - Oxford, N.Y., 1976) p. 483.

15. P.J. Turchi, A.L. Cooper, R. Ford and D.J. Jenkins, Phys. Rev. Lett. 36, 1546 (1976).

16. C.A. Kapetanakos, R.K. Parker and K.R. Chu, Appl. Phys. Lett. 26, 284, (1975).

17. E. Fermi, Nuclear Physics (Univ. of Chicago Press, Chicago, 1950) p. 36.

18. D.A. Hammer, C.A. Kapetanakos and N. Ury, J. Appl. Phys. 44, 1121 (1973).

19. C.A. Kapetanakos, J. Golden and F.C. Young, Nuclear Fusion, 16, 151 (1976).

20. M.J. Clauser, Phys. Rev. Lett. 35, 848 (1975).

21. J.W. Shearer, Nucl. Fusion 15, 952 (1975).

22. S. Yoshikawa, Phys. Rev. Lett. 26, 295 (1971).

23. J.D. Sethian, K.A. Gerber, D.N. Spector and A.E. Robson, Phys. Rev. Lett. 41, 798 (1978).

24. C.A. Kapetanakos, J. Golden and K.R. Chu, Plasma Physics 19, 387 (1977).

25. J.D. Lawson, J. Electron. Contr. 3, 587 (1957); 5, 146 (1958); J. Nucl. En. Pt. C, 1, 31, (1959).

26. D.A. Hammer and N. Rustoker, Phys. Fluids 13, 1831 (1970).

27. H.S. Uhm and R.C. Davidson, Phys. Fluids 22, (1979).

28. C.A. Kapetanakos, Phys. Fluids 22, No. 5 (1979).

29. R.C. Davidson, Theory of Nonneutral Plasmas (W.A. Benjamin, Inc., Reading, Mass.) 1974.

Table 1

Source

Average hollow beam radius at the anode (cm)	26
Magnetic Field (kG)	2.3
Pulse Duration (nsec)	70

Compression Region

	Before Compression	After Compression
Proton energy (MeV)	2	100
Magnetic field at M.P. (kG)	18.2	910
Proton current (MA)	0.92	46
Number of protons	2×10^{17}	2×10^{17}
Ring kinetic energy (MJ)	0.064	3.2

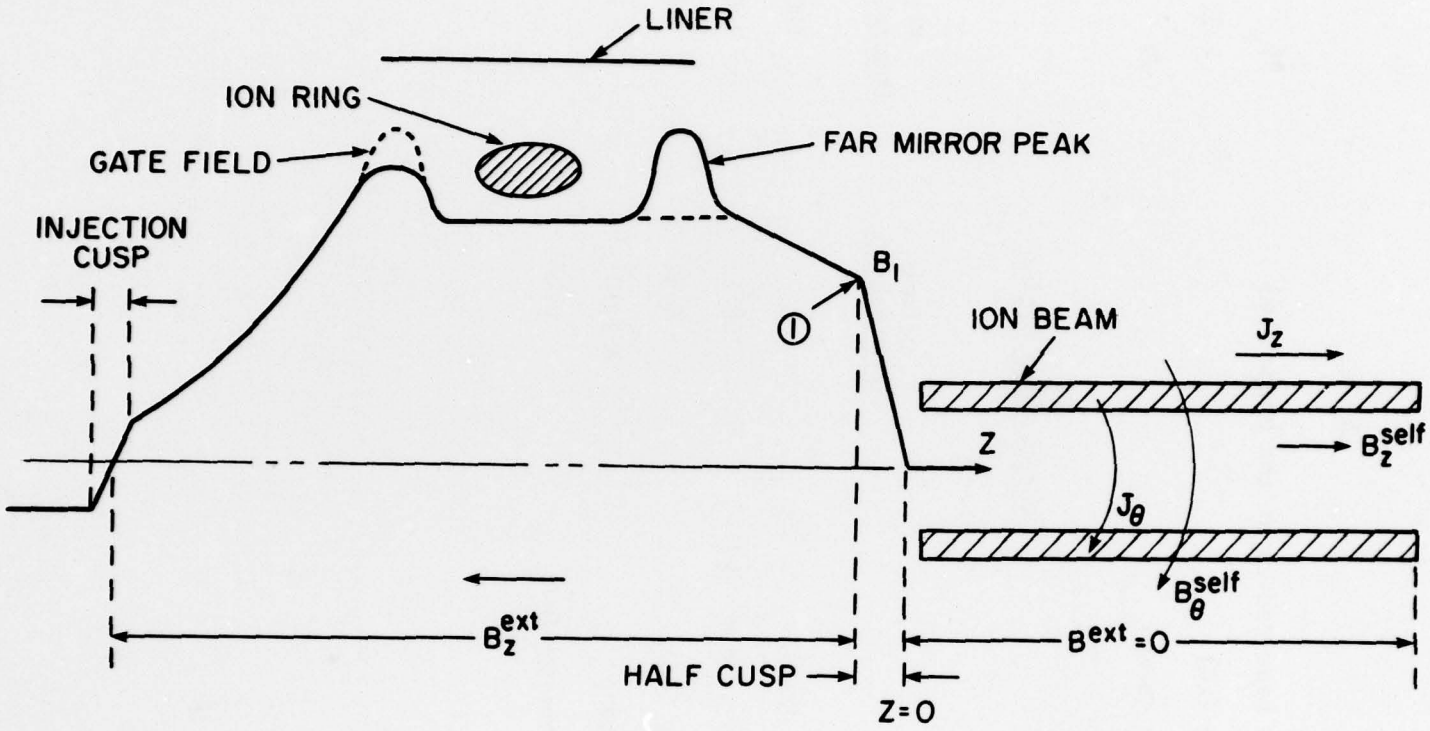

Fig. 1 — Illustration of the magnetic field configuration for the generation of high energy ion pulses

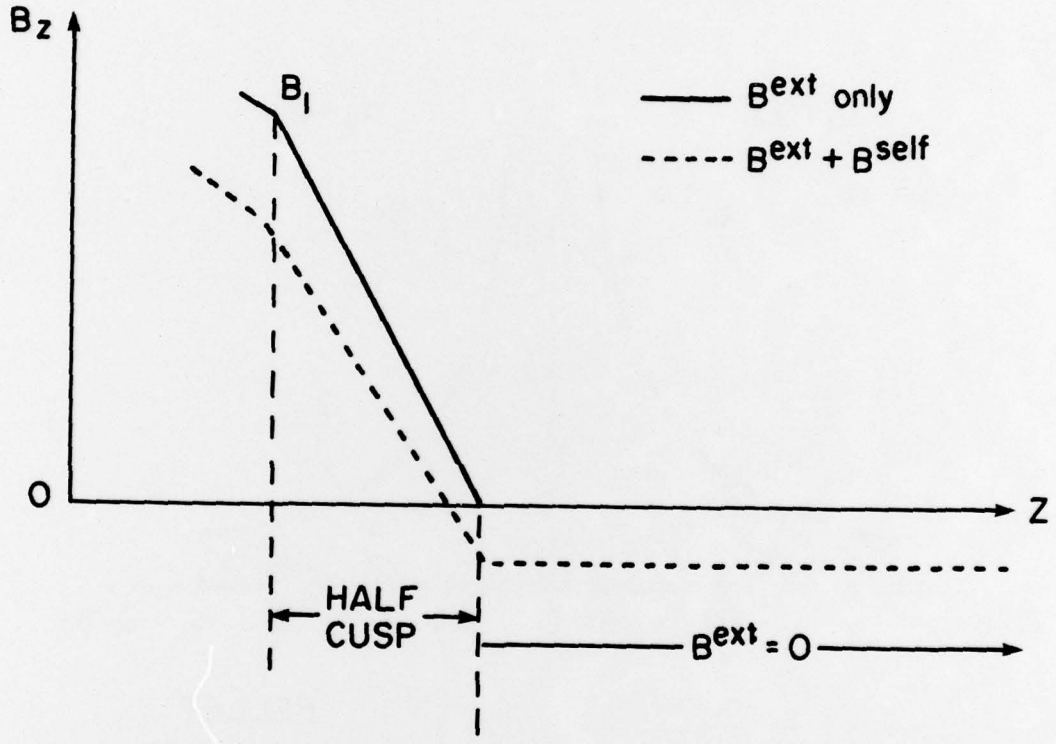

Fig. 2 — Illustration of the effect of the self magnetic field of a rotating beam on a linear half cusp

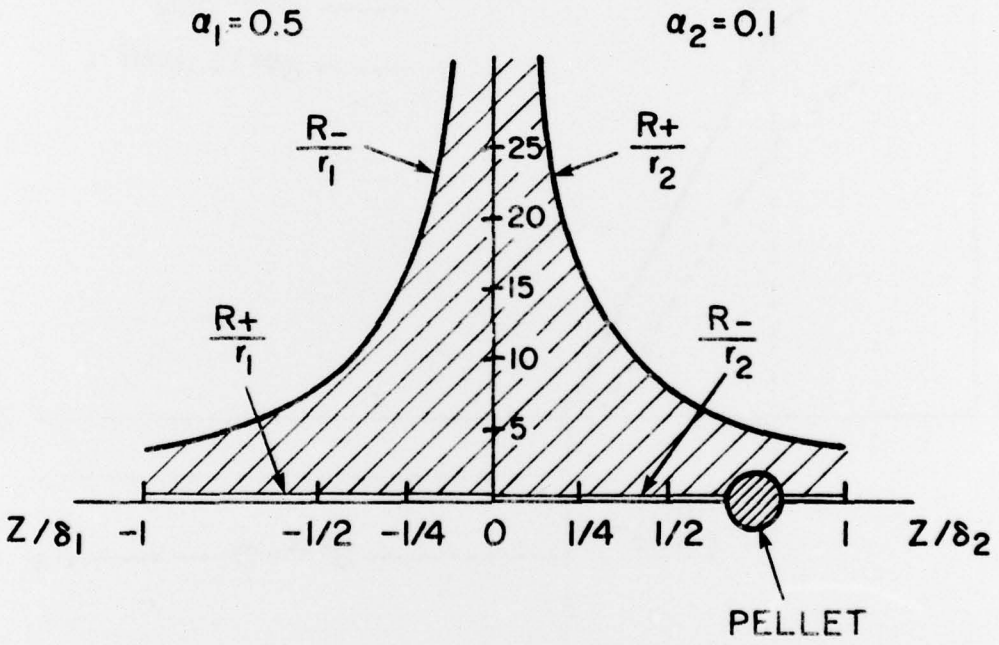

Fig. 3 — Boundary of the allowed region (hatched) of a full cusp when $a_1 = 0.5$ and $a_2 = 0.1$

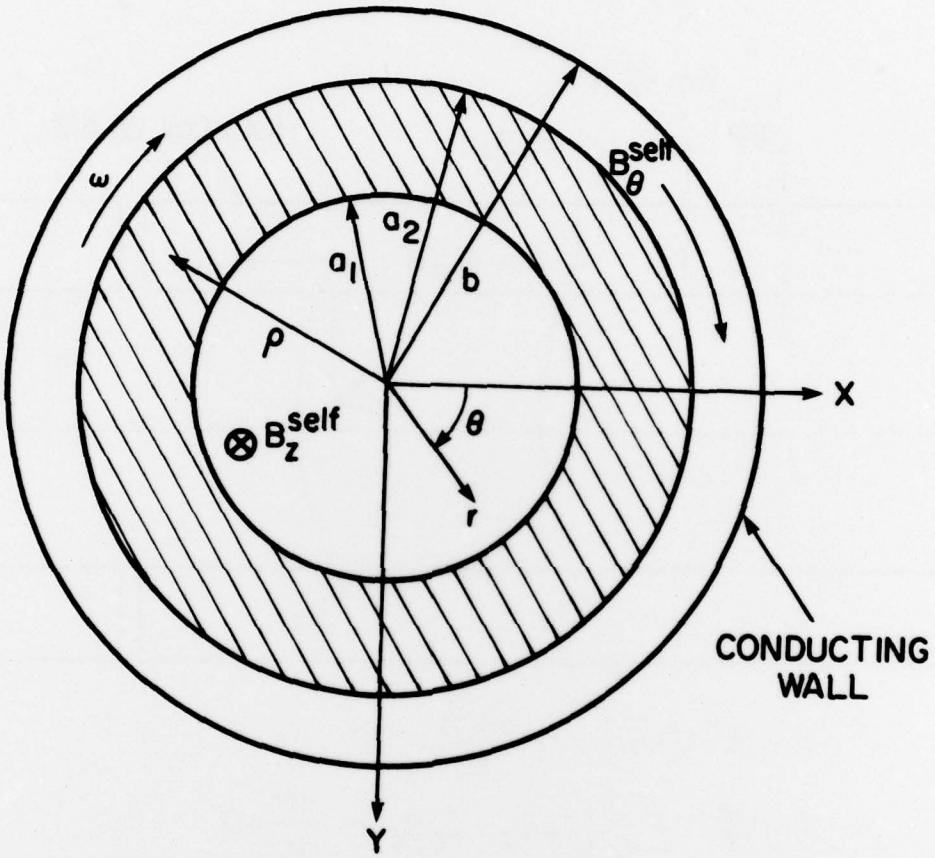

Fig. 4 — Equilibrium configuration and coordinate system

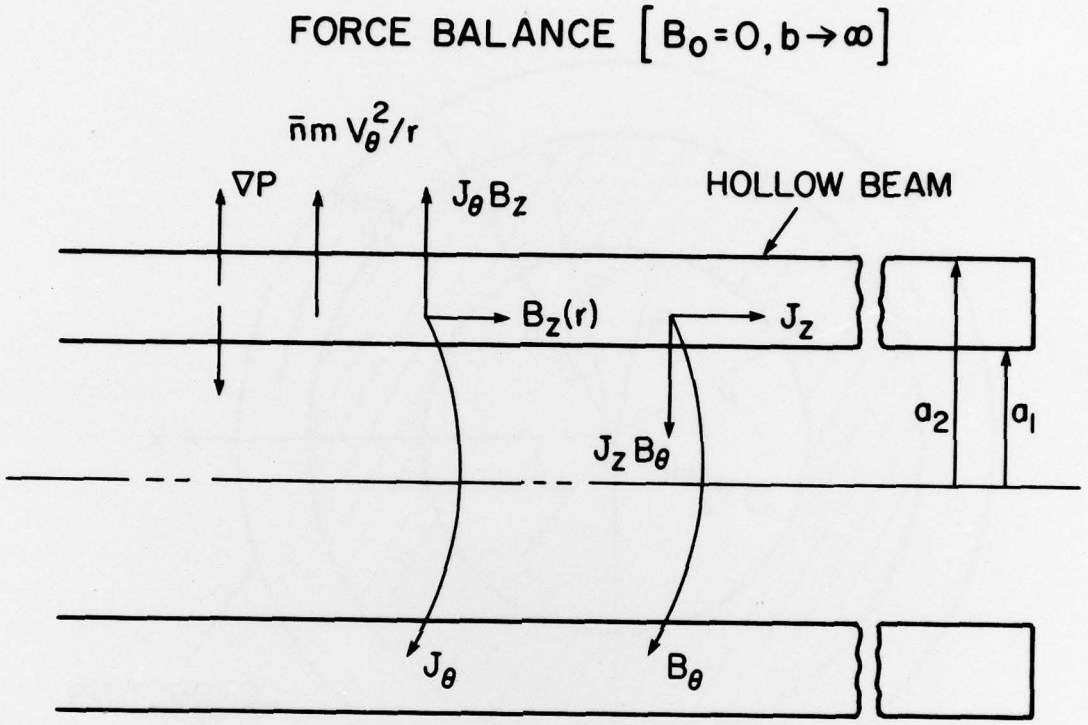

$$\bar{n}m(\bar{V}\cdot\nabla)\vec{V} = \bar{n}q\frac{\vec{V}\times\vec{B}}{C} - \nabla P$$

$$\bar{n}mV_\theta^2/r + \frac{1}{C}\left[J_\theta B_z - J_z B_\theta\right] - \frac{dP}{dr} = 0$$

Fig. 5 — Illustration of various forces acting on the beam

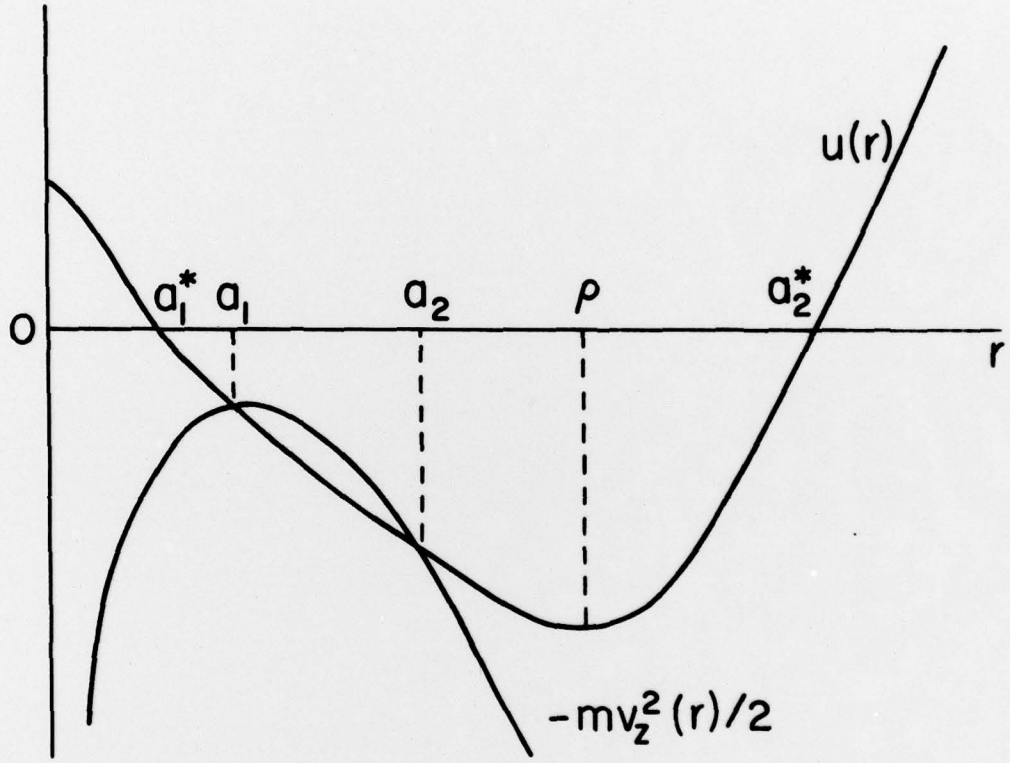

Fig. 6 — Sketch of functions U(r) Eq. (43) and $-mv_z^2(r)/2$ Eq. (44) vs. radial distance. The intersections of two curves give the inner a_1 and outer a_2 radii of the beam.